Tomographic reconstruction of the ionosphere using generalized singular value decomposition

K. Bhuyan, S. B. Singh and P. K. Bhuyan*

Department of Physics, Dibrugarh University, Dibrugarh 786 004, India

The total electron content (TEC) of the ionosphere, being the line integral of the electron density encountered by a transionospheric wave along its path of propagation, does not convey any information about the structures within the ionosphere. In recent years, computer-aided ionospheric tomography (CIT) has been increasingly used for the investigation of electron density distribution in the low and mid-latitude ionosphere. A number of CIT algorithms have been proposed, but they have their individual shortcomings. In this communication, we present a new algorithm based on generalized singular value decomposition technique (GSVD). The algorithm was tested with TEC data generated using the International Reference Ionosphere (IRI-1995) model for the Indian low latitudes and measured by the Global Positioning System satellites along a chain of European mid-latitude stations. The reconstructed images using the GSVD technique have been found to match well with the model and the measured data.

THE ionospheric total electron content (TEC) has been measured for many years now using the Faraday rotation and differential Doppler techniques. These measurements provide information about the temporal and spatial variation of TEC. Multistation TEC data have been used to study the horizontal (latitudinal as well as longitudinal) variation of ionospheric structure. However, since TEC represents the integral of the electron density along the path, the information about the spatial variation of electron density along the path caused by the irregular structures cannot be recovered using conventional techniques. Austen *et al.*[1] demonstrated the feasibility of using the computerized tomography technique to successfully reconstruct ionospheric structures from TEC data. Computerized tomographic (CT) technique can be used when the line integral of the parameter to be determined (e.g. electron density) is the measured data through the region of interest. CT technique has had a revolutionary impact in the field of medical diagnostic imaging and is now routinely used to produce high quality images of a section of the human body. The technique has also been applied to the study of ocean structures[2] and geological formations[3]. The success of tomographic technique in medical diagnostics is well known[4]. The mathematical foundation of the CT was laid as early as 1917 by Radon (Deans[5]).

*For correspondence. (e-mail: bhuyan@dibru.ernet.in)

Raymund *et al.*[6] applied the computerized ionospheric tomography (CIT) to realistically simulate the ionospheric electron density variations over 16° in latitude within a height range of 50 to 1000 km. In a CIT experiment, the line-integrated electron density (TEC) is measured simultaneously along various paths in a plane in the ionosphere using a number of stations that receive beacon signals from a rapidly orbiting satellite. The plane is gridded into small areas or pixels and the electron density assumes a constant value within each pixel. The TEC measurements can then be used to reconstruct the electron density distribution in the vertical plane between the satellite and ground receivers.

The relatively recent development of inexpensive, high-speed computers has made tomography a more readily accessible tool for remote sensing; in particular for imaging the electron density in the earth's ionosphere, and the number of CIT algorithms has increased rapidly in recent years. Some of them are, the algebraic reconstruction technique (ART)[1], the multiplicative algebraic reconstruction technique (MART)[6–8], maximum entropy method (MEM)[9,10], etc. Raymund[11] has made a comparative assessment of various CIT algorithms and observed that no single algorithm can be considered as the best. Some algorithms that construct well in one case do poorly in other cases. Some algorithms do well in parts (e.g. bottom-side gradients), but poorly at others. It was also observed that the fundamental assumptions make significant differences and proper choice of the algorithm will be the prime requisite for meaningful data reconstruction. The ART and MART algorithms are conceptually simple and computationally efficient, which make them good general-purpose CIT algorithms. The ART algorithm used to reconstruct the images seeks to minimize the root mean square difference between the observed TEC data and those computed from the reconstruction. The ART algorithm is iterative and requires some starting image as an initial guess. The algorithm computes the root mean squared difference at each iteration and then makes additive changes that seek to minimize the difference. In many ways, MART is similar to ART. It is also iterative and starts from an initial guess. It compares TEC computed from the initial guess with the measured TEC. At each iteration, changes to the image are based on the difference. Of course, the difference with ART is that the changes are multiplicative rather than additive. The MEM algorithm uses two alternating iterative procedures.

Tomography is a part of the family of inverse problems. The difficulty with inverse problems is that they are often ill-posed. Such problems are characterized by (1) instability, (2) non-existence and (3) non-uniqueness of the solution. They are best handled with the discrete inverse theory. In this communication, the development of a new algorithm based on generalized singular value decomposition (GSVD) has been discussed.

The TEC of the ionosphere is defined as the number of free electrons contained in a column of unit cross-section area. In mathematical form, it can be represented as,

$$\text{TEC} = \int_p n(s)\, ds,$$

where $n(s)$ is the electron density and p is the propagation path between the satellite and the receiver. Under the discrete inverse theory approach, TEC along some path p_i can be approximated as a finite sum of integrals along shorter path segments of p_i. The electron density is discretized into a set of N pixels $\{x_j\}$, x_j being the electron density in the jth pixel.

Let $\{y_i\}$ be the set of TEC measurements where i refers to a given path. Also, a basis function $B_{ij}(s)$ is defined such that,

$B_{ij}(s)$ = constant, if the jth pixel is intersected by p_i at s.

= 0, otherwise.

The basis function can be obtained from a standard ionospheric model such as International Reference Ionosphere (IRI). For the sake of simplicity, the constant has a value of 10^5 in our case, the unit of electron density (electrons cm^{-3}) inside each pixel (as obtained from IRI).

The approximation of TEC as a sum of shorter path integrals can be written as,

$$y_i = \int_{p_i} n(s)\, ds = \sum_{j=1}^{N} x_j \int_{p_i} B_{ij}(s)\, ds,$$

where y_i is the TEC along the path p_i.

Let

$$P_{ij} = \int_{p_i} B_{ij}(s)\, ds.$$

Once the geometry has been chosen, the length of the path segments P_{ij} can be calculated and stored as an array A_{ij}.

The reconstruction problem then centres on solving the system of equations:

$$y_i = \sum_{j=1}^{N} A_{ij} x_j + e_i,\ i = 1, 2, 3, \ldots, M,$$

or,

$$y_{M\times 1} = A_{M\times N} x_{N\times 1} + e_{M\times 1},$$

where M is the number of ray paths and N the number of pixels. y is obtained from TEC data and x is the unknown electron density distribution.

The loss of information and inconsistency of data make ionospheric tomography an ill-posed inverse problem. Such problems are best handled with the generalized approach of singular value decomposition (SVD). The GSVD is a generalization of the SVD technique, that can be used to solve the damped least squares problem as proposed by Tikhonov[12]. This approach amounts to finding out the x that solves

$$\min_{x\in R^N} \| Ax - y \|^2 + \alpha^2 \| Lx \|^2,$$

where α is the regularization parameter and $\alpha > 0$. L is a positive definite matrix which takes different forms according to the order of regularization. For zeroth-order Tikhonov regularization, $L = I$, the identity matrix and for first-order Tikhonov regularization

$$L = \begin{pmatrix} -1 & 1 & 0 & . & . & 0 \\ 0 & -1 & 1 & 0 & . & 0 \\ . & . & . & . & . & . \\ . & . & . & . & . & . \\ 0 & . & . & 0 & -1 & 1 \end{pmatrix},$$

where L is a $P \times N$ matrix.

Under GSVD technique, the matrices $A_{M\times N}$ and $L_{P\times N}$ with $M \geq N \geq P$, and rank $(L) = P$, can be written as

$$A = U \begin{pmatrix} \Lambda & 0 \\ 0 & I_{N-P} \end{pmatrix} B^{-1},$$

and

$$L = V(C\ \ 0)B^{-1},$$

where U is $M \times N$ and orthogonal, V is $P \times P$ and orthogonal, and B is $N\times N$ and non-singular. Λ is $P \times P$ diagonal matrix with elements λ_i such that

$$0 \leq \lambda_1 \leq \lambda_2 \leq \lambda_3 \leq \lambda_4 \ldots \leq \lambda_P \leq 1.$$

C is a $P \times P$ diagonal matrix with elements μ_i such that

$$1 \geq \mu_1 \geq \mu_2 \geq \mu_3 \geq \mu_4 \ldots \geq \mu_P > 0.$$

The Tikhonov regularized solution can be written as

$$x_{\alpha,L} = (A^T A + \alpha^2 L^T L)^{-1} A^T y.$$

In the damped least square approach, the value of α is unspecified. The indeterminacy of α can be eliminated by the method of generalized cross validation (GCV).

Let

$$G(\alpha) = \frac{\| Ax_{\alpha,L} - y \|^2}{\text{Trace}(I - AA^{\#}_{\alpha,L})^2} = \frac{V(\alpha)}{T(\alpha)}.$$

Table 1. Reconstruction geometry

Number of ray paths	90
Number of pixels	84 (6 rows and 14 columns)
Altitude range	100–600 km
Latitude range	16°N–22.5°N
Vertical dimension of one pixel	100 km
Horizontal dimension of one pixel	55 km (~ 0.5° in latitude)
Number of receivers	3, 5

Here $V(\alpha)$ measures the misfit. As α increases, $V(\alpha)$ also increases. $T(\alpha)$ is a slowly increasing function of α. A regularization parameter α is selected, for which $G(\alpha)$ has a minimum value. We have used the MATLAB[13] regularization toolbox function 'gcv' to calculate the regularization parameter.

Table 1 represents the geometry used for the reconstruction. TEC has been simulated along 90 different ray paths from the electron density distribution obtained from the International Reference Ionosphere (IRI-95). Figure 1 illustrates the electron density distribution for 11 March 2002 at 1200 h LT along 75°E meridian, as obtained from IRI-95. The reconstructed electron density distribution is plotted in Figure 2. The regularization parameter α has a value of 1.28E-06 in the 5-receiver case. It is seen that the equatorial ionization anomaly is reconstructed particularly well. The tilt of the ionosphere is also well preserved. Figure 3 represents the reconstructed electron density distribution for a 3-receiver geometry. The reconstruction geometry is same as that in the 5-receiver case.

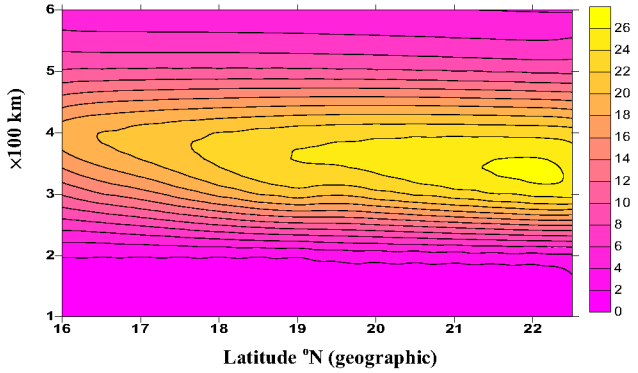

Figure 1. Contour plot of electron density (in units of 10^5 electron/cm^3) distribution in an altitude versus latitude plane over Indian low latitudes as obtained from the IRI-95.

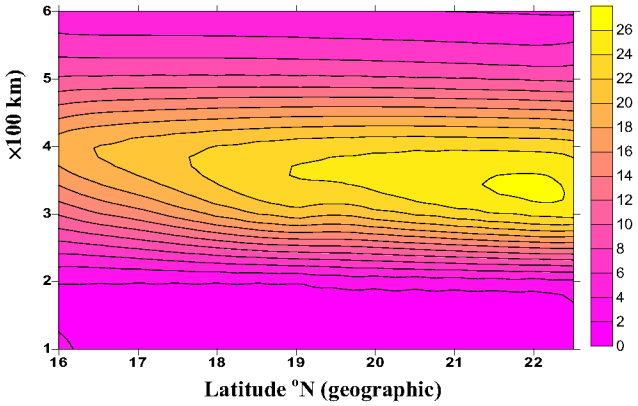

Figure 2. Contour plot of reconstructed electron density (in units of 10^5 electron/cm^3) distribution in the same altitude versus latitude frame obtained for a 5-receiver geometry.

It is seen that the reconstruction is not much affected; only the electron density values in the bottommost row of pixels are slightly different from those obtained for the previous case. The regularization parameter α has a value of 5.62E-07 in this case.

Table 2 shows the norm of the misfit between the electron density distribution obtained from IRI-95 and the reconstructed electron density distribution (5-receiver case) for the pixels at different altitudes. The norm of the misfit is found to be 8.36E-01 for all the solutions. It has been noted that the maximum contribution to the misfit comes from the topmost (at 600 km altitude) and the bottommost (at 100 km altitude) rows of pixels, the misfit at all the other altitudes being negligible.

The algorithm has also been used for the reconstruction of experimental TEC data obtained from the Chilbolton Weather Web (www.rcru.rl.ac.uk/weather/tec.htm). Vertical TEC has been scaled for nine stations covering 16.8° in latitude along 15 ± 6°E meridian at 1200 h LT. Slant TEC was simulated for 90 different ray paths spanning a gridded region of 84 (6 rows × 14 columns) pixels. The horizontal dimension of each pixel is 165 km; the vertical dimension being 100 km. Table 3 gives the receiver position, the measured vertical TEC and the reconstructed vertical TEC for all the nine stations. The

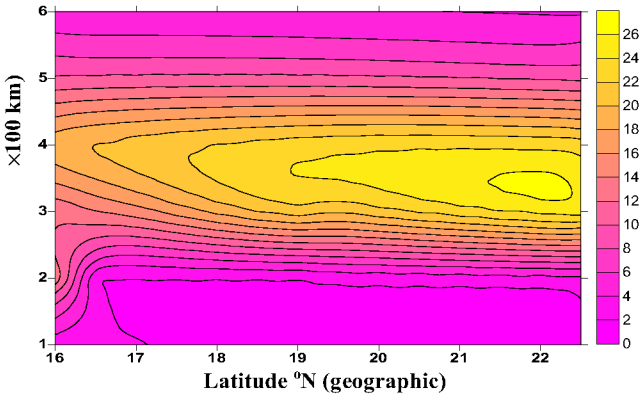

Figure 3. Contour plot of reconstructed electron density (in units of 10^5 electron/cm^3) within the altitude latitude configuration as in Figures 1 and 2 for a 3-receiver geometry.

Table 2. Norm of the misfit between IRI electron density and reconstructed electron density

Altitude (km)	Norm of the misfit
600	1.85 E-01
500	1.17E-04
400	1.18E-04
300	8.19E-05
200	8.66E-05
100	8.15E-01

Table 3. Receiver position, measured vertical TEC, reconstructed vertical TEC and difference between measured and reconstructed vertical TEC

Receiver number	Latitude °N, (geographic)	Station	Longitude (°E)	Vertical TEC (TECU#)	Reconstructed TEC (TECU)	ΔTEC (%)* (± TECU)
1	40.6	Matera	16.7	78.62	77.38	+ 1.58
2	44.5	Medicina	11.6	70.56	69.77	+ 1.12
3	47.1	Graz	15.5	62.22	63.98	– 2.83
4	47.3	Innsbruck	11.4	66.11	63.98	+ 3.22
5	49.1	Koetzting	12.9	59.17	59.46	– 0.49
6	52.3	Borowiec	17.1	45.52	52.02	– 14.27
7	52.4	Potsdam	13.1	56.55	52.02	+ 8.01
8	53.9	Olsztyn	20.7	48.61	50.82	– 4.55
9	57.4	Onsala	11.9	56.21	55.67	+ 0.96

TECU = Total Electron Content Unit (10^{16} el. m^{-2}).
*ΔTEC = [(Vertical TEC – Reconstructed vertical TEC)/Vertical TEC] × 100.

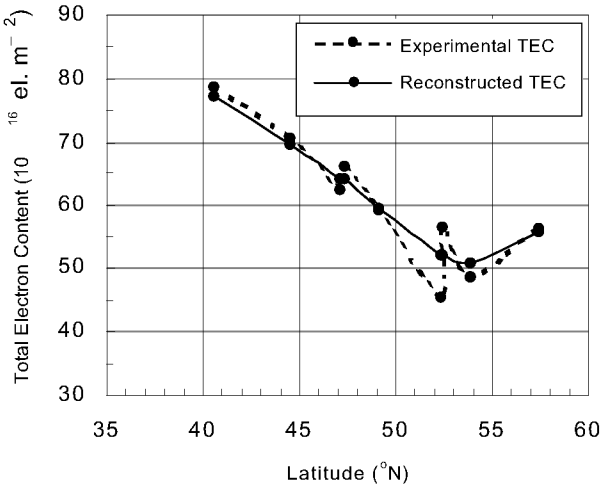

Figure 4. Comparison between the experimental and reconstructed vertical TEC at European mid-latitudes.

experimental TEC and the reconstructed TEC are plotted in Figure 4. The difference in measured TEC between two very closely situated stations may be because of the separation in longitude between the two. There is also the possibility of the reconstructed TEC being averaged out because the two stations lie within the same pixel. It should be noted that the GSVD approach requires that the number of ray paths (i.e. the TEC values) should exceed the number of pixels.

In the reconstruction process, it is assumed that the ray paths lie well within the gridded region. The error in the measurement of TEC may cause erroneous reconstruction of the electron density distribution. Of course, with the increasing accuracy in TEC measurements, e.g. the error in TEC measurement by GPS satellites being minimized to ~ 1 TECU, the proposed algorithm is expected to perform particularly well in reconstructing the ionospheric structures. It is observed that the number of receivers plays an important role in the reconstruction process. Increasing the number of receivers enhances the quality of the reconstructed image.

1. Austen, J. R., Franke, S. J.and Liu, C. H., *Radio Sci.*, 1988, **23**, 299–307.
2. Munk, W. and Wunch, C., *Deep Sea Res.*, 1979, **26A**, 123–161.
3. Dines, K. A. and Lyttle, R. J., *Proc. IEEE*, 1979, **67**, 1065–1073.
4. Yeh, K. C. and Raymund, T. D., *Radio Sci.*, 1991, **26**, 1361–1380.
5. Deans, S. R., *The Radon Transform and some of its Applications*, John Wiley, New York, 1983.
6. Raymund, T. D., Austen, J. R., Franke, S. J., Liu, C. H., Klobuchar, J. A. and Staker, J. S., *Radio Sci.*, 1990, **25**, 771–789.
7. Kersely, L., Heaton, J. A. T., Pryse, S. E. and Raymund, T. D., *Ann. Geophys.*, 1993, **11**, 1064–1074.
8. Bust, G. S., Cook, J. A., Kronschnabl, G. R., Vasicek, C. J. and Ward, S. B., *Int. J. Imaging Syst. Technol.*, 1994, **5**, 160–168.
9. Fougere, P. F., *Radio Sci.*, 1995, **30**, 429–444.
10. Fremouw, E., Howe, B., Secan, J. and Bussey, R., *Int. J. Imaging Syst. Technol.*, 1994, **5**, 97–105.
11. Raymund, T. D., *Ann. Geophys.*, 1995, **13**, 1254–1262.
12. Tikhonov, A. N., *Sov. Math. Dokl.*, 1963, **4**, 1035–1038.
13. Hansen, P. C. and IMM, MATLAB regularization toolbox, version 3.1, September 2001.

ACKNOWLEDGEMENTS. This work is partially supported by the Indian Space Research Organisation (ISRO). K.B. is grateful to ISRO for providing him a JRF.

Received 9 May 2002; revised accepted 18 September 2002